Development of LGADs and AC-LGAD at BNL and neutron detection

G. D'Amen[1], W. Chen[1], G. Giacomini[1], L. Lavitola[2], S. Ramshanker[3], A. Tricoli[1]
[1]Brookhaven National Laboratory (US)
[2]Universita' degli studi Federico II (IT)
[3]Oxford University (UK)

BROOKHAVEN NATIONAL LABORATORY

19 November 2019

Outline

Time resolution - **LGAD**

I. Introduction to LGADs
II. LGAD response to ^{90}Sr β^-
III. LGAD interaction with fast neutrons
IV. Comparison with Geant4 simulation

Space & time - **AC-LGAD**

V. The AC-LGAD concept & fabrication
VI. Tests with IR, red laser and ^{90}Sr

Conclusions and Future activities

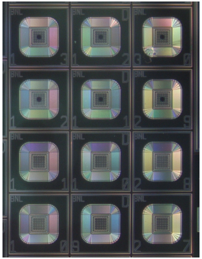

LGAD wafer (BNL)

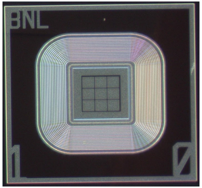

AC-LGAD matrix (BNL)

Low Gain Avalanche Diode

Introduction

Low Gain Avalanche Diode (LGAD): highly doped layer of p-implant (**Gain layer**) near p-n junction creates a high electric field that accelerates electrons enough to start multiplication.

- Electric Field: ~300 kV/cm in Gain Layer
- Silicon-based technology with low, adjustable gain (2 - 100)
- Breakdown Voltage ∝ Gain parameters (dose, energy)
- High Signal/Noise ratio
- Ability to achieve fast-timing $\mathcal{O}$(20-30) ps in high radiation environments

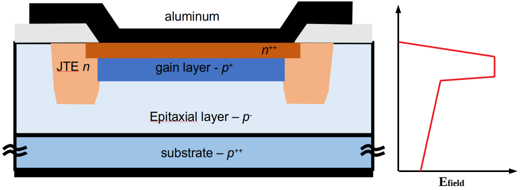

Questions to be answered:

- MIPs detection capabilities already proven, fast neutron response to be characterized
- How fast is the response to fast neutrons?
- What are out limits of detectable neutron energy?

LGAD structure

Wafer structure (W1836,W1837,W1840)

- 1×1 mm^2 sensor size
- 50 μm ^{28}Si p epitaxial layer, ^{10}B and ^{11}B doped ($7 \times 10^{13} cm^{-3}$)
- Different doping concentrations (3, 3.25 and 2.7 $\times 10^{13} cm^{-3}$) and gain layer thickness

- 500 μm substrate
- Aluminum thin layer
- Silicon Oxide SiO_2
- n++ layer, ^{31}P doped
- Gain p+ layer, ^{11}B doped

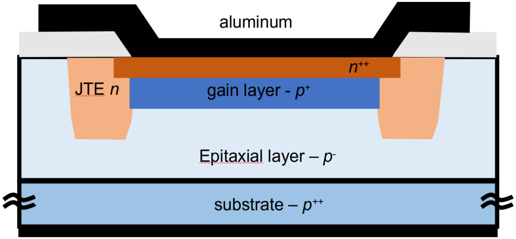

^{90}Sr interactions

Signal waveforms

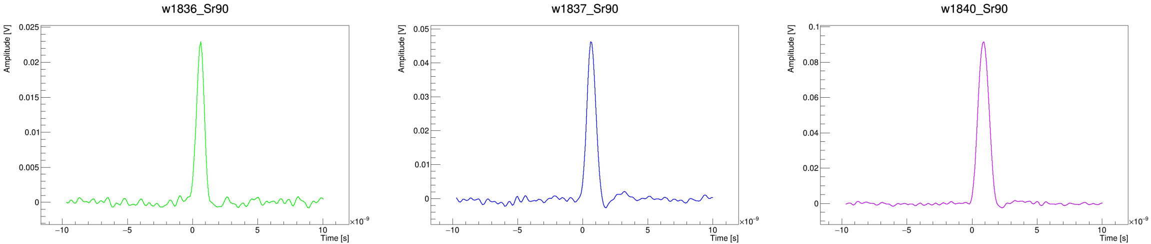

Waveforms from β^- ^{90}Sr signals

- **W1836**, **W1837**, **W1840** show narrow peaks with widths $\mathcal{O}(1\text{ ns})$
- Sensors Gain for β^- compatible to that of X-rays
- $\sigma_{jitter} \approx$ 20ps

	Sensor Gain (X-Ray):
W1836:	~ 15
W1837:	~ 20
W1840:	~ 25

Deuterium-Tritium neutron generator

BNL Thermo-Fisher MP 320 Neutron Generator (prototype)

$$^{3}T +^{2} D \rightarrow^{4} He + n(14.1\ MeV) \tag{1}$$

Neutron energy spectrum very narrow $\sigma_E = \mathcal{O}(10^{-2}$ MeV) and isotropic, with estimated neutron production of 6×10^{7} neutrons/sec, with a flux of 7×10^{4} neutrons/(cm^2 sec) at sensor position

Fast Neutron interactions

Signal waveforms

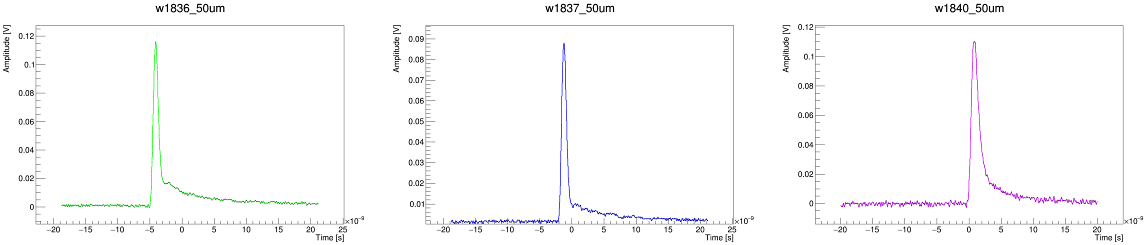

Waveforms from neutron signals

- Trigger = 10 mV
- **W1836**, **W1837**, **W1840** show narrow peaks with widths $\mathcal{O}(1\text{ ns})$
- Sensor Gain for neutrons compatible to the one measured with X-rays

	Sensor Gain (X-Ray):
W1836:	~ 15
W1837:	~ 20
W1840:	~ 25

Fast Neutron interactions

Deposited Energy distributions

Energy deposited by the neutron interaction computed as integral of each signal:

$$E_{dep}\ [eV] = \frac{3.6\ [eV]}{G_n\ R_{fb}\ q_e} \int_{wf} A dt$$

Good agreement with gain measure with X-ray in the "*sensitive*" range in deposited energy ($\propto (G_n)$), limited by **trigger voltage** and **maximum signal amplitude** in oscilloscope window.

For a **10 mV trigger** level and $G_n = 15$, sensitivity to neutron signals with deposited energy as low as $\sim$ **30 keV**.

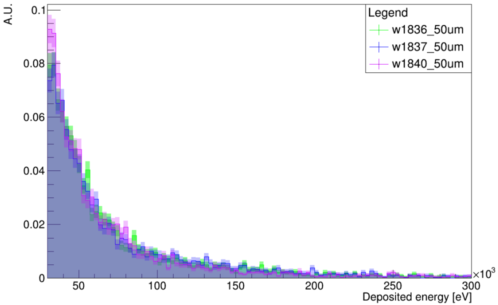

Fast Neutron interactions

Jitter measurement

Jitter is an important component of the time resolution of the sensor; computed as ratio between the noise (∼0.5 mV for all the sensors) and slew rate (dV/dt):

$$\sigma_j = \langle \sigma_{noise} \left(\frac{dV}{dt} \right)^{-1} \rangle \sim 20\ ps$$

Slew rate (normalized)

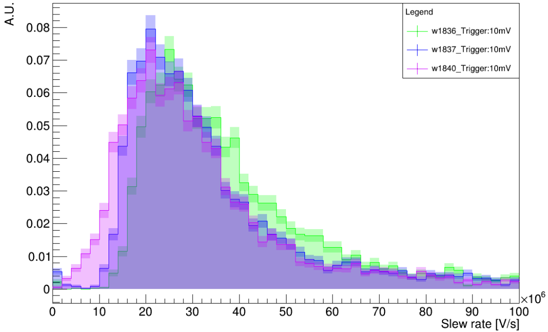

Generated energy spectrum

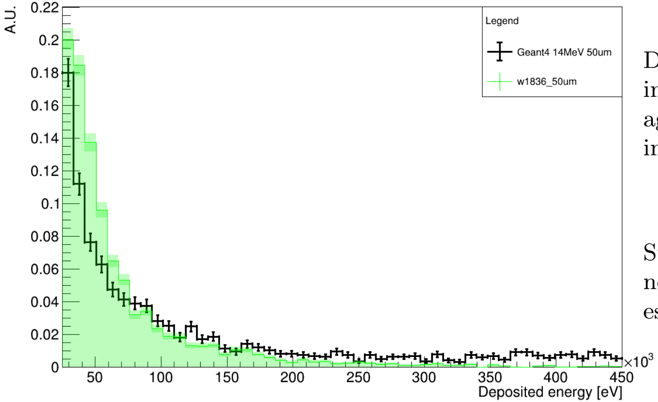

Distribution of energy deposited by neutron interaction as simulated by Geant4 shows good agreement with experimental data from **W1836** in the sensor sensitive range $E_{dep} = [30, 450]$ keV

Superimposing E_{dep} distributions generated by neutrons with different energies can give us an estimate of minimum neutron energy sensitivity

Neutron energy sensitivity

Extrapolation of sensitivity to various neutron energies based on 14.1 MeV data

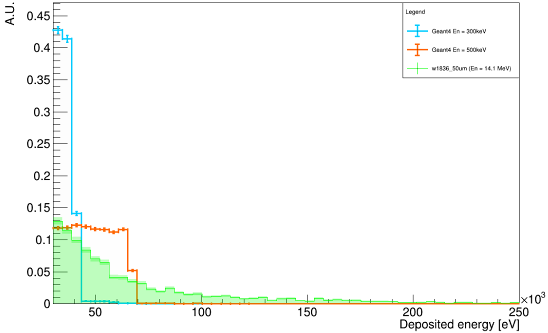

W1836 sensitivity (according to 14.1 MeV deposited E distribution) to **300-** and **500-** keV neutrons

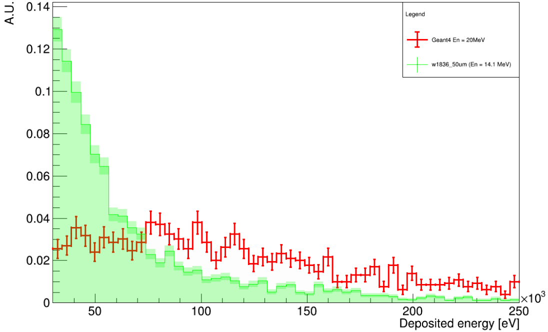

W1836 sensitivity (according to 14.1 MeV deposited E distribution) to 20 MeV neutrons

Near future plans

- Validate simulation for lower energy neutron with ^{252}Cf source (already available at BNL) $\rightarrow$ neutron emitter @ 2 MeV.

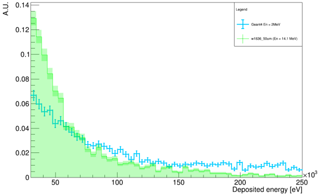

- Lower trigger threshold from 10 mV to 2 mV (×4 average noise); expected sensitivity to $E_n < 100$ keV:

- E_{dep} **th @10mV**
  W1836: ~30 keV
  W1837: ~20 keV
  W1840: ~22 keV
- E_{dep} **th @2mV**
  W1836: ~6 keV
  W1837: ~4 keV
  W1840: ~4 keV

- Testing AC-LGAD response to DT (14.1 MeV) and ^{252}Cf (2 MeV) neutrons

The **AC-LGAD** concept

- Limits of LGADs
- The AC-LGAD concept
- Fabrication of AC-LGADs @ BNL

Limits of LGADs

Lateral dimensions of Gain layer must be much larger than thickness of substrate, to create uniform multiplication.
Dead volume (local gain ∼ 1) extends within the implanted region of the gain layer:

- Pixels/strips (pitch ∼ 100 mm) with gain layer below the implant have a Fill Factor «100% (Voltage dependent)
- Large pads (∼ 1 mm) are preferred (e.g. ATLAS HGTD or CMS MTD)
- Good for timing, hardly for 4D reconstruction
- Various possible ways to overcome this issue with different geometries

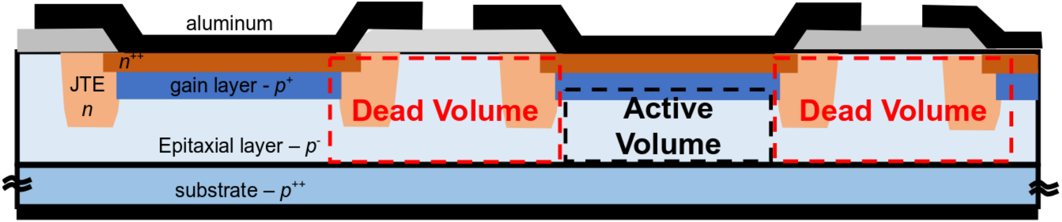

AC-LGAD

concept

Main differences w/r to LGADs:

1. One large low-doped high-ρ n^+ implant running overall the active area, instead of a high-doped low-ρ n^{++}
2. Thin insulator over the n^+, where fine-pitch electrodes are placed, patterned over the insulator

Expected Results:

- $\sim$ 100% Fill Factor and fast timing information at a per-pixel level achieved
- Signal generated by drift of multiplied holes into the substrate but AC-coupled through dielectric
- Electrons collect at the resistive n^+ and then slowly flow to a ohmic contact at the edge.

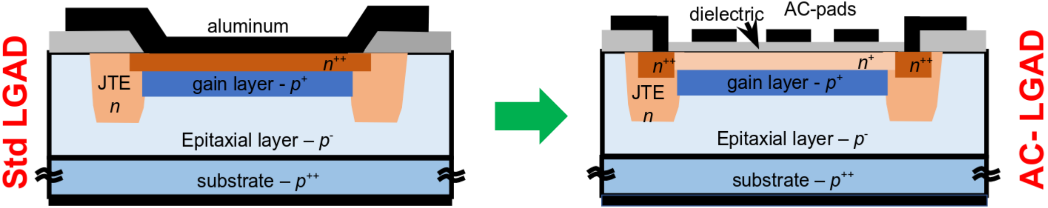

AC-LGAD

Fabrication at BNL

Process:

- Process starts from a Std (DC-) LGAD **Pad**
- Change METAL (*Aluminum*) and thus Contacts
- n^{++} runs at the periphery only; replaced by resistive n^{+} in the active area with 10/100 less dose
- Thin insulator (100 nm SiN) over the n^{+}

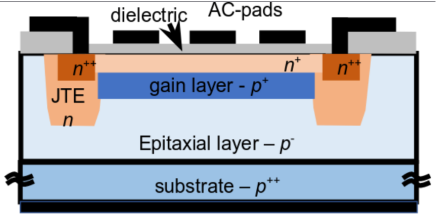

Std-LGAD **Pad:**

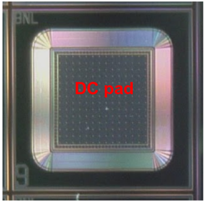

AC-LGAD **Pixels:**

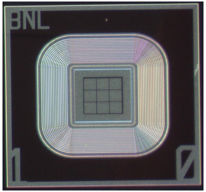

AC-LGAD **Strips:**

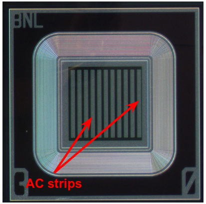

AC-LGAD characterization

Recalibration of gain layer

In the very first AC-LGADs wafers, used the same gain layer dose as in LGADs.
Problem: the n^+ is little doped, and its depleted thickness is not negligible; the p^+ gain layer is deeper, leading to lower Breakdown Voltage.

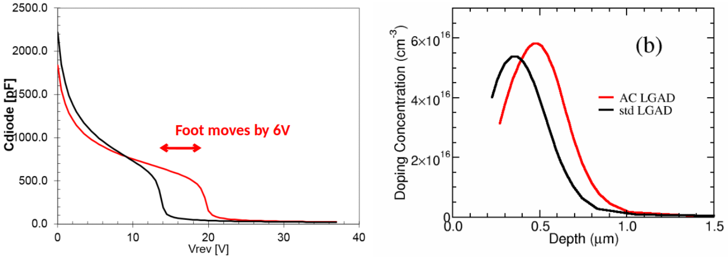

Gain layer dose has been lowered in following production, while keeping the process flow very similar.

Tests with IR, red laser and ^{90}Sr

- LGAD vs AC-LGAD comparison
- Cross-Talk studies
- Timing performance

AC-LGAD

Signal comparison with LGADs

- Sensor wire-bonded to 16 channel Trans-impedance Amplifier board by FermiLab
- **AC-LGAD:** 3×3 pixel matrix, 200μm × 200μm AC-coupled pads bonded to TAs
- **LGAD:** same AC-LGAD device where the n^{++} is read-out by the TA (same bias conditions and gain)

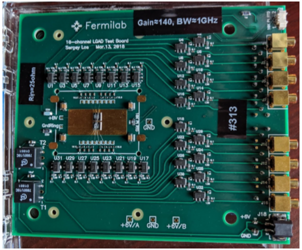

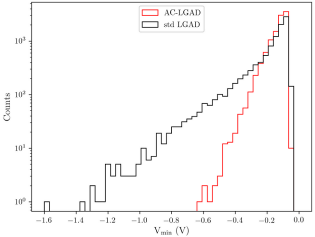

- Comparison of pulse amplitudes of betas from ^{90}Sr.
- Essentially equal distribution (same gain) for LGAD and AC-LGAD Amplitudes
- All signal goes through C_{AC} = 20pF
- Is this signal well spatially localized? Need to estimate Cross-Talk between pixels/strips

Cross-talk

Pixel Map

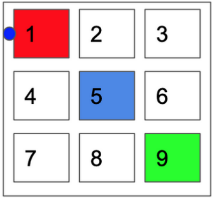

Cross-talk measured as ratio between signal amplitude peaks in different pixels

	Dose n$^+$ 1/10	**Dose n$^+$ 1/100**
ratio A5/A1	9%	17%
ratio A9/A1	16%	11%

Response of a single pixel as a function of shining position of IR or red laser (TCT scan).

Border effect: the n^{++} is a low resistance path that couples the signals back to the pixel under measure.

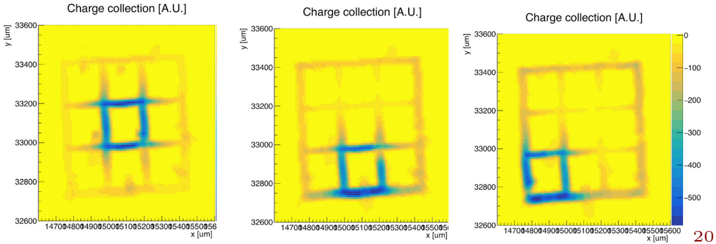

Cross-talk

Strip Map

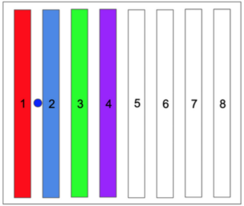

Response of a single strip as a function of shining position of IR or red laser (TCT scan).

Border effect: the n^{++} is a low resistance path that couples the signals back to the strip under measure.

Cross-talk measured as ratio between signal amplitude peaks in different strips

	Crosstalk
ratio A2/A1	100%
ratio A3/A1	13%
ratio A4/A1	6%
ratio A6/A1	4%

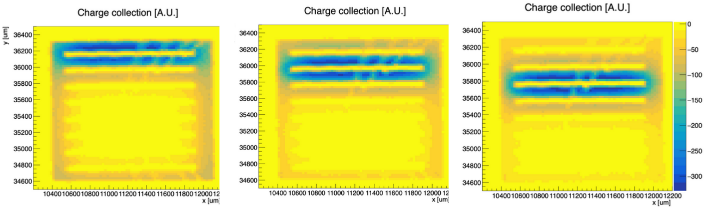

Timing Resolution

- AC-LAGDs and LGADs show similar response (waveforms)→ expected ∼ same **timing performance**
- Using beta signals from a ^{90}Sr source on AC-LGADs lead to estimated σ_{jitter} ∼20 ps
- **NEXT:** Measuring timing resolution in coincidences with a trigger sensor, using 3D-printed **Beta Scope** setup ready with ∼ 180 MBq ^{90}Sr source
- Developed a setup such that our probe station can operate both at room temperature and at -30°C which will be used for pre/post irradiation IV and CV scans

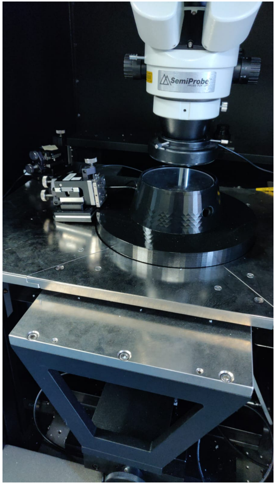

Conclusions

LGADs can be used to detect neutrons in the 100s keV - MeV (and beyond?) energy range in **high flux** conditions for applications where **fast time** ($\sim$20 - 30 ps) measurements are needed

Fast timing for fast neutrons ensured by **jitter** measurement of $\mathcal{O}(15 - 20)$ ps

Good agreement between data and G4 simulation; extrapolations from Geant4 simulations shows potential **sensitivity** to neutrons with energies $<$100 keV

By changing a few photolithographic masks and tuning process flow parameters, **AC-LGADs** have been fabricated as well

Precision **space resolution** (50-100 μm) available with AC-LGAD technology

Cross-talk and **time resolution** tested with mips and TCT, leading to positive results

Additional info/links

- G. Giacomini, W. Chen, F. Lanni, and A. Tricoli, *Development of a technology for the fabrication of Low-Gain Avalanche Diodes at BNL*
- G. Giacomini, W. Chen, G. D'Amen, A. Tricoli, *Fabrication and performance of AC-coupled LGADs*

Backup

Motivation

Low-Gain Avalanche Diodes (LGAD) are gathering interest in the Physics community thanks to fast-timing and radiation-hardness:

- **HEP:** ATLAS (HGTD) and CMS (MTD) timing detectors at the HL-LHC
- **NASA:** neutron flux studies
- **Medical Imaging:** PET scans
- **Quantum information, Nuclear and forward physics**, etc...

MIPs detection capabilities already proven, investigating the response to neutrons in the $\mathcal{O}$(MeV) region (fast neutrons)

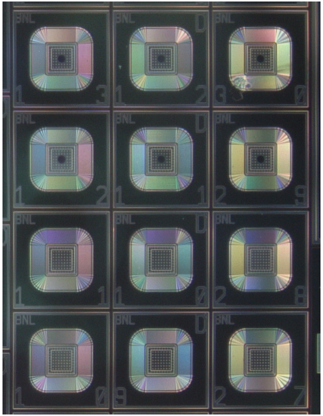

Wafer of LGADs produced at BNL

Sensor gain computation

Signals max amplitude

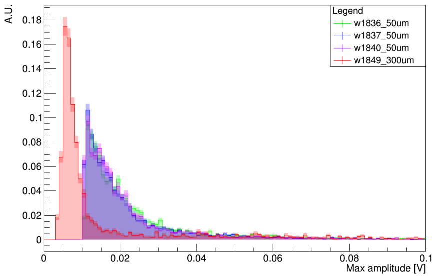

Distributions of maximum signal amplitude (*left*) are divided by the sensor gain G_n (*right*), as obtained from X-ray measurements.

Max amplitude scaled by Gain (normalized)

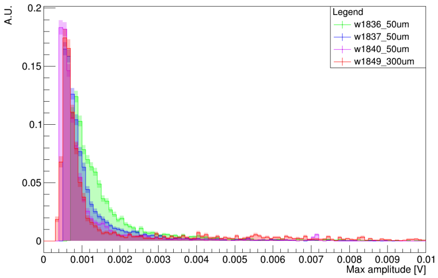

- **Sensor Gain:**

  W1836: ~ 15

  W1837: ~ 20

  W1840: ~ 25

Slew Rate

Average signal Noise

- W1836: (0.39±0.54) mV
- W1837: (0.10±0.43) mV
- W1840: (0.19±0.5) mV
- W1849: (-0.11±0.42) mV

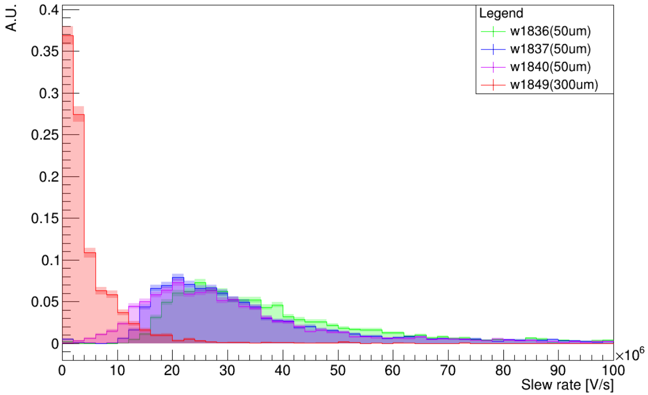

Sensitive range

Full width at half maximum (normalized)

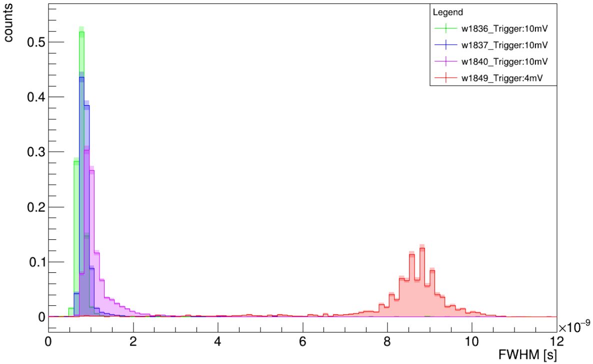

Sensitive region limited by trigger voltage (10 mV for W1836, W1837, W1840, 3.5 mV for W1849) and maximum signal amplitude in oscilloscope window.

Energy distributions constrained in region between:

$$I_{th} = \sqrt{2\pi}\, V_{th}\, \frac{\langle FWHM \rangle}{2.355}$$

with V_{th}^{min} = trigger level and V_{th}^{max} = max window amplitude

LGAD fabrication at BNL

- 4âĂİ p-type epitaxial wafers (100), NA $\leq 1\times10^{14}\text{cm}^{-3}$, 50mm thick($V_{depl}$ $\sim$120V). Also FZ used.
- 4 ion implantations (JTE and gain at high energy)
- 6 photolithographic masks
- p-spray isolation (patterned externally to the active area to avoid implant on gain region).
- Little thermal drive-in (mainly for the JTE âĂŞJunction Termination Edge for protection from high Eat the border of the shallow n+implant)
- layout with pads of 1x1 mm^2, 2x2 mm^2, 3x3 mm^2 and arrays.

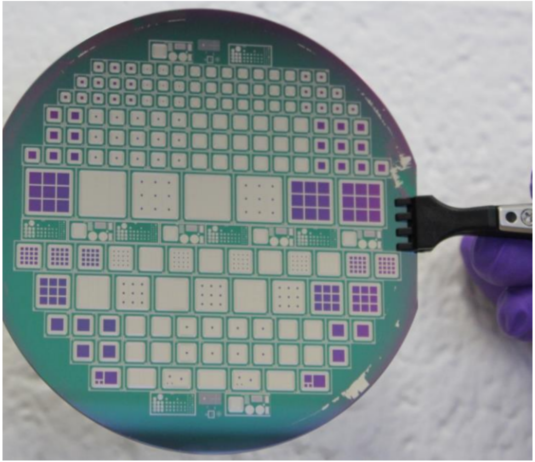

Low Gain Avalanche Diode

LGAD production @ BNL

Silicon Fabrication Facility and wire- and bump- bonding @ *BNL Instrumentation Div.*, full characterization, design and simulation of silicon sensors @ *Si-Lab*

- Leakage current (measured on diodes) for 1x1 mm^2 of $\sim$ 10 pA (1 nA/cm^2)
- Consistent from batch to batch
- Clearly current depends on gain layer dose, so does the breakdown voltage
- GR can stand higher voltages

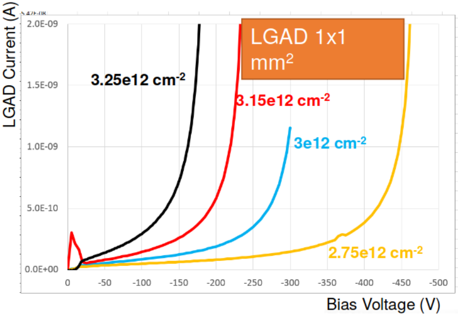

LGAD structure

Thin device 50μm (W1836,W1837,W1840)

- 1×1 mm^2 sensor size
- 50 μm ^{28}Si p epitaxial layer, ^{10}B and ^{11}B doped ($7\times10^{13} cm^{-3}$)
- different doping concentrations (3, 3.25 and 2.7 $\times10^{13} cm^{-3}$) and gain layer thickness
- 500 μm substrate

Thick device 300μm (W1849)

- 3×3 mm^2 sensor size
- 300 μm ^{28}Si p- substrate, ^{10}B and ^{11}B doped ($5\times10^{11} cm^{-3}$)
- sensor volume $\sim$54 times bigger than 50μm devices

Wafer structure

- Aluminum thin layer, thickness 0.5 μm
- Silicon Oxide SiO_2, thickness 0.3 - 0.5 μm
- n++ layer, ^{31}P doped, thickness 0.5 μm
- Gain p+ layer, ^{11}B doped, thickness 0.5 μm

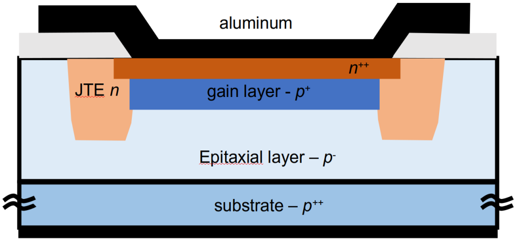

Signal waveforms

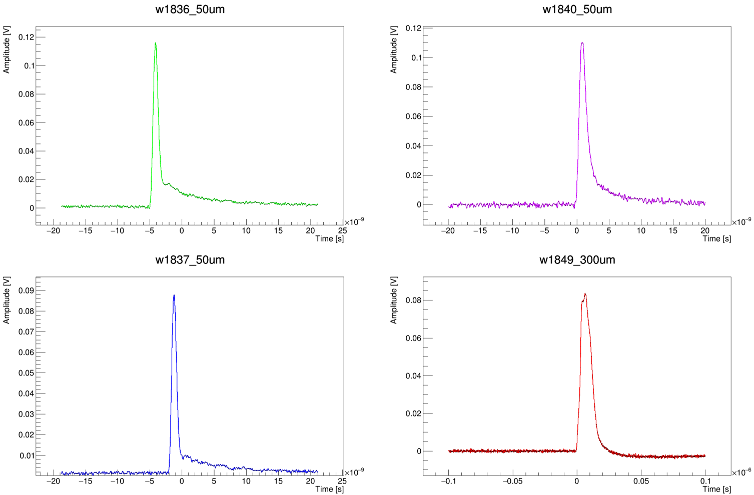

Waveforms acquired with *Tektronix MSO64* mixed-signals oscilloscope;

W1836, W1837, W1840 (50 μm) show narrow peaks with widths $\mathcal{O}$(1 ns), while W1849 (300 μm) produces longer ($\sim$ 8 times) signals.

Sensor gain computation

Signals max amplitude

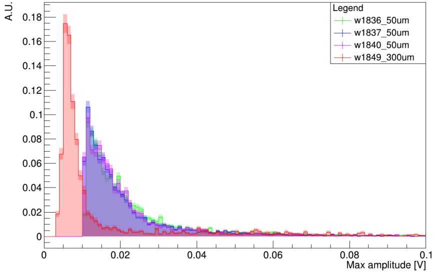

Max amplitude scaled by Gain (normalized)

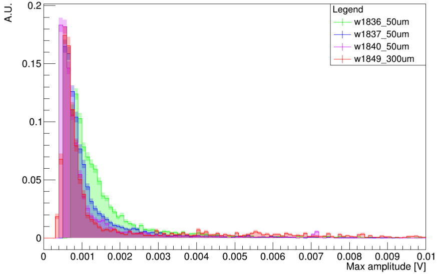

Distributions of maximum signal amplitude (*left*) are divided by the sensor gain G_n (*right*), as obtained from X-ray measurements.

- **50 μm Gain:**
  W1836: $\sim$ 15
  W1837: $\sim$ 20
  W1840: $\sim$ 25
- **300 μm Gain:**
  W1849: $\sim$ 10

Jitter measurement

Jitter is an important component of the time resolution of the sensor and is computed as ratio between the noise (∼0.5 mV for all the sensors) and slew rate (dV/dt):

$$\sigma_j = \langle \sigma_{noise} \left(\frac{dV}{dt} \right)^{-1} \rangle$$

Sensor	Gain	Jitter [ps]
W1836:	∼15	14.8 ± 3.6
W1837:	∼20	17.5 ± 4.3
W1840:	∼25	21.3 ± 4.3
W1849:	∼10	222.4 ± 42.7

Slew rate (normalized)

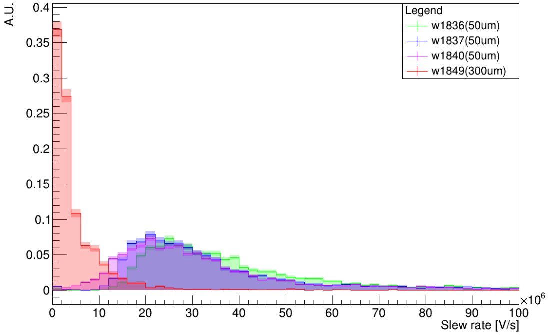

Deposited Energy distributions

300 μm sensor comparison

W1849 (300μm) has been compared to the 50 μm sensors:

- Compatible shape in the sensitive range after gain correction
- Higher detection efficiency ($\times$54 times volume)
- Different minimum threshold of sensitive range:
  E_{dep}^{min} =$\sim$ **30keV** (50μm) vs $\sim$ **200keV** (300μm)

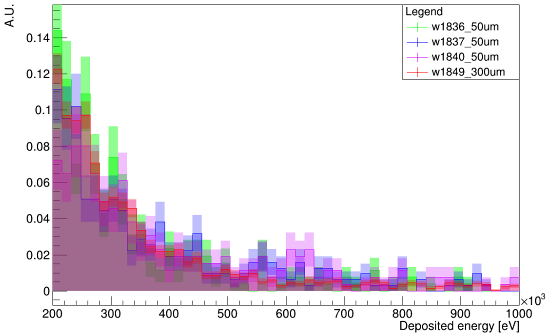

Characterization of neutron processes

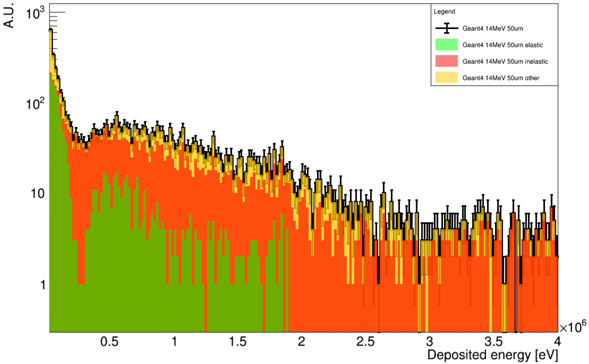

- **Neutron Elastic** interaction significant for 14 MeV neutron interactions with deposited energy up to $\sim$ 1.85 MeV
- **Neutron Inelastic** interaction dominant contribution for high deposited energies
- In the range E_{dep} = [30, 450] keV minimal contributions from photons and electrons **electromagnetic processes** (ionization, Compton effect, photoelectric effect) and **decays**

Scan of neutron energy sensitivity

Distributions of deposited energy for neutrons with:

- $K = 10/100$ keV (*top-left*)
- $K = 200/300$ keV (*top-right*)
- $K = 500/700$ keV (*bottom-left*)
- $K = 1$ MeV (*bottom-right*)

for Trigger threshold 10 mV and $G_n = 15$, expected sensitivity to 300 keV neutrons

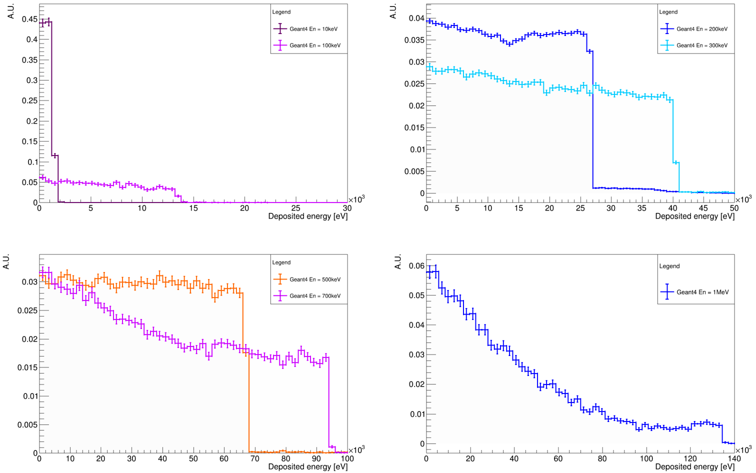

LGAD STRUCTURE

Wafer structure (W1836,W1837,W1840)

- 1×1 mm^2 sensor size
- 50 μm ^{28}Si p epitaxial layer, ^{10}B and ^{11}B doped ($7 \times 10^{13} cm^{-3}$)
- Different doping concentrations (3, 3.25 and 2.7 $\times 10^{13} cm^{-3}$) and gain layer thickness
- 500 μm substrate
- Aluminum thin layer, thickness 0.5 μm
- Silicon Oxide SiO_2, thickness 0.3 - 0.5 μm
- n++ layer, ^{31}P doped, thickness 0.5 μm
- Gain p+ layer, ^{11}B doped, thickness 0.5 μm

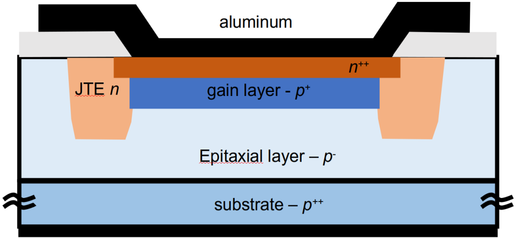

GEANT4 SIMULATION

INTRODUCTION

Sensor response modelled with GEANT4 10.4 MonteCarlo simulation software

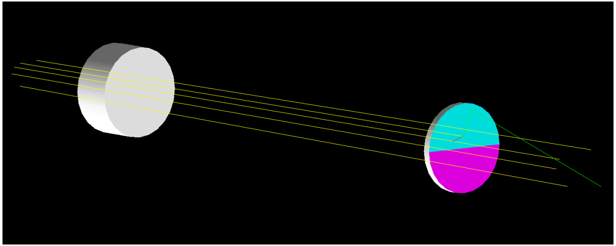

Simulation parameters:

- QGSP_BIC_HP physics list used for high precision simulation of neutrons ≤ 20 MeV
- 10 million 14.1 MeV neutrons generated each simulation run with randomized initial direction
- 1.6 mm of ^{27}Aluminum interposed between neutron generator and sensor, to simulate the Deuterium-Tritium generator casing

AC-LGAD characterization

IV-curve